Austrian Journal of Earth Sciences | Vienna | 2017 | Volume 110/2 | xxx - xxx | DOI: 10.17738/ajes.2017.0015

Spatial and temporal analysis of recent seismicity in different parts of the Vlora-Lushnja-Elbasani-Dibra Transversal Fault Zone, Albania

Rrapo ORMENI[1)], Serkan ÖZTÜRK[2)*)], Akli FUNDO[3)] & Kemal ÇELIK[4)]

[1)] Institute of Geosciences, Energy, Water and Enivornment Polytechnic University, Tirana, Albania;

[2)] Gümüşhane University, Department of Geophysics, TR-29100, Gümüşhane, Turkey;

[3)] Polytechnic University, Tirana, "Nene Tereza" square, Albania;

[4)] Gümüşhane University, Department of Geomatics Engineering, TR-29100, Gümüşhane, Turkey;

[*)] Corresponding author, serkanozturk@gumushane.edu.tr

KEYWORDS Albania; Vlora-Lushnja-Elbasani-Dibra Fault Zone; *b*-value; fractal dimension; precursory seismic quiescence; earthquake potential

Abstract

Spatial and temporal evaluation of current seismic activity throughout the Vlora- Lushnja-Elbasani-Dibra (VLED) transversal fault zone were carried out at the beginning of year 2016. The seismotectonic b-value, fractal dimension *Dc*-value and precursory seismic quiescence *Z*-value are considered for a detailed statistical analysis. Completeness magnitude *Mc*-value varies from 2.5 to 2.7 for different parts of the VLED fault zone. The *b*-value is calculated as 1.10±0.04 for the south western part and 1.13±0.05 for the middle part, whereas it is estimated as 0.94±0.07 for the north eastern part of the study region. These results reveal that *b*-values for all regions are well represented by a *b*-value typically close to 1.0. There are clear decreasing trends in temporal changes of *b*-values before the occurrences of some strong main shocks. On the contrary, no earthquakes are observed in some periods after decrease of *b*-value. *Dc*-values are computed as 2.66±0.04 for the south western part, 2.64±0.03 for the middle part and 2.15±0.02 for the north eastern part of the VLED fault zone. These rather large values show that earthquake activity is more clustered at larger scales or in smaller areas in the study area.

Considering the phenomenon of seismic quiescence as a precursor of the main earthquakes gives successful outcomes in defining the potential anomalies and possible locations of future earthquakes. Quiescence analysis of current seismicity at the beginning of 2016 in the VLED fault zone is performed with the test of standard normal deviate *Z*-value. Distributions of resulting *Z*-values show six anomalous regions along the different parts of the VLED fault zone. These quiescence areas are detected at (*i*) 40.81°N-19.86°E (including Kuc-Bubullim, southeast of Lushnja town), (*ii*) 41.00°N-20.01°E (in the Cerriku, south of Elbasani town), (*iii*) 41.31°N-20.13°E (around Bene-Qafe, northeast of Elbasani town), (*iv*) 41.43°N-20.21°E (Krasta-Batra, south of Bulqiza town), (*v*) 41.28°N-20.49°E (including Carrishta-Stebleve, northeast of Librazhdi town), (*vi*) 41.51°N-20.51°E (including Qerrenec-Gjorica, west of Dibra town). As an important result, analyses of spatial and temporal characteristics of the earthquake activity may supply significant clues for revealing the future seismic hazard along the VLED fault zone, and these anomaly regions may be interpreted as the locations of next possible earthquakes.

1. Introduction

There exist a lot of regional and temporal studies on the space-time characteristics of earthquake activity for different parts of the world, and many authors obtained important outcomes and conclusions by using scaling laws (e.g., Utsu, 1971; Mandelbrot, 1982; Habermann, 1983; Hirata, 1989; Frohlich and Davis, 1993; Wiemer and Wyss, 2000; Awad, 2005; Öztürk et al., 2008; Öncel and Wilson, 2007; Roy et al., 2011; Öztürk, 2011; 2015; Ali, 2016). The Albania region is seismically active with tens of destructive large earthquakes over the past twenty centuries as revealed from the historical sources (Sulstarova et al., 1980; Ormeni, 2010). Albania is located at the Alpine-Mediterranean seismic belt and accommodates part of the deformation due to the collision of the Adriatic microplate with the Eurasian plate (Mazzoli and Helman, 1994). The main reason of seismicity in Albania is the collision of the Adriatic microplate forming the Albanian orogen. This continental collision directly influences the inner part of the country, along longitudinal and transverse faults cutting across the eastern and the north-eastern part of Albania (Aliaj et al., 2001; Ormeni et al., 2013).

The Vlora-Lushnja-Elbasani-Dibra (VLED) transversal fault zone in Albania is a major tectonic feature with a well-defined fault trace and an established history of seismicity. Major earthquake activity of the VLED fault zone during the 20th century began with the destructive Peshkopia earthquake in 1920 in northeast Albania and migrated westwards by a series of destructive earthquakes in 1921, 1930, 1935, 1942, 1959, 1962, 1967, 1982, 2009, 2014 and 2015 (Sulstarova et al., 1980; Aliaj et al., 2001; Ormeni, 2015). Current tectonics of Albania is represented by a significant micro-seismicity, small and medium-sized events and a few large earthquakes as given by the occurrence of six main shocks with *Ms* magnitudes exceeding 6.0 throughout the last century (Kociaj, 1986): June 1, 1905 Shkodra earthquakes (*Ms*=6.6), February 18, 1911 Ohrid Lake earthquake (*Ms*=6.7), November 26, 1920 Tepelena earthquake (*Ms*=6.4), December 17, 1926 Durres earthquake (*Ms*=6.2),

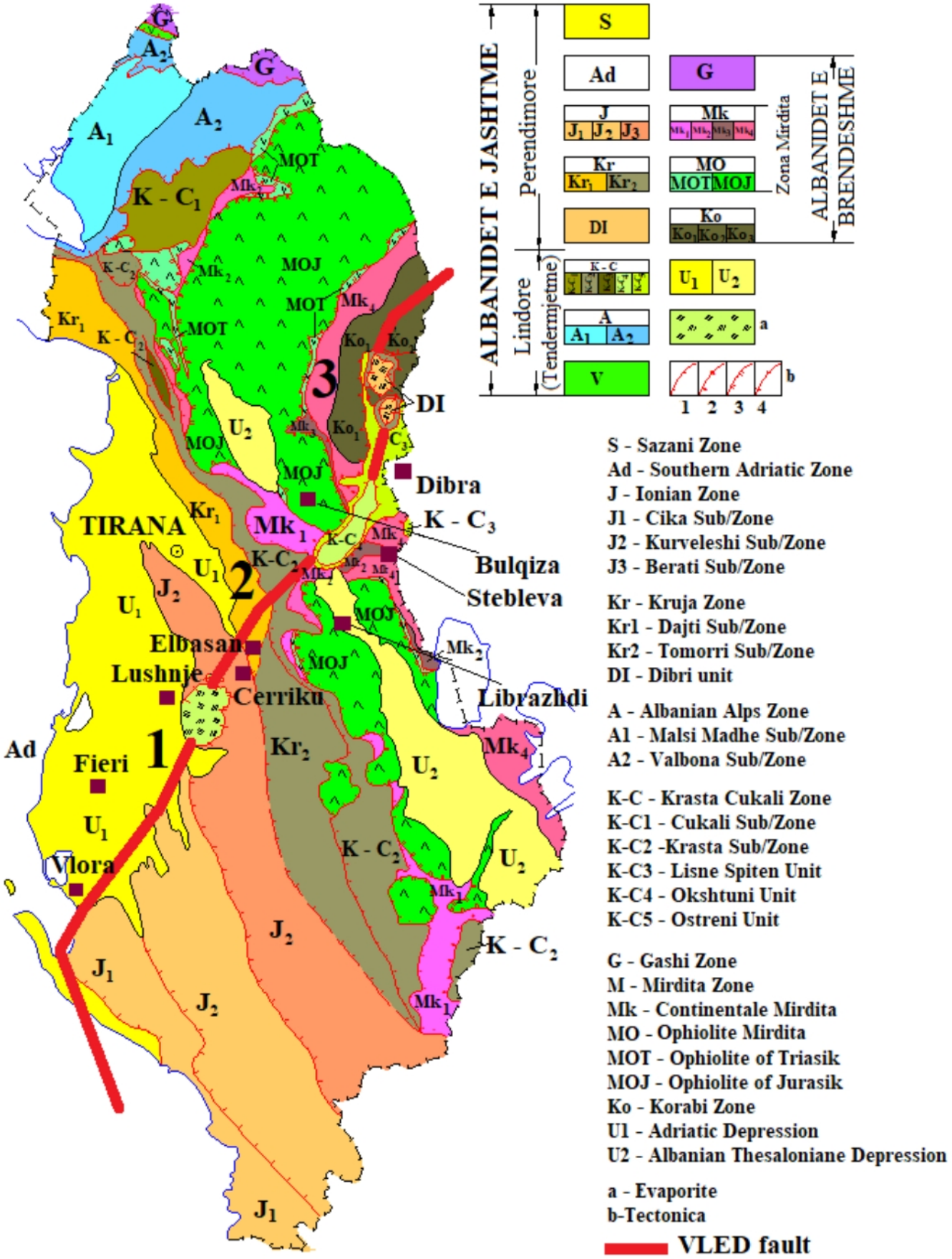

Figure 1: Schematic tectonic structure of Albania and seismic source zones in the VLED Transversal Fault Zone. Zones are marked: 1- (Vlora-Lushnje) South western part of VLED, 2- (Elbasani) Middle part of VLED, 3- (Dibra) North eastern part of VLED. Names of tectonic structures: Vlora and Lushnja flexure (VLF), Dumrea diapire dome (DDD), Elbasani Quaternary depression (EQD), Labinoti transversal structure (LTS), marked by important Quaternary infill (Melo, 1986), Golloborda transversal horst (GTH) continues toward the Tetova Quaternary Graben (TQG).

November 30, 1967 Dibra earthquake (*Ms*=6.6) and April 15, 1979 Montenegro earthquake (*Ms*=6.9). In recent years, however, three strong earthquakes occurred along the VLED fault zone: September 6, 2009 (M_L=5.4), the Gjorica earthquake which occurred in the eastern Albania - the former Yugoslav Republic of Macedonia (FYROM) border, May 19, 2014 (M_L=5.2), the Cerrik earthquake which was near Elbasan, and November 1, 2015 (M_L=5.0), the Bulqize earthquake which is located 34 km east of the capital city Tirana (Ormeni et al., 2013).

In the scope of this study, we analyzed the spatial and temporal behaviors of the earthquakes along the VLED fault zone in order to evaluate the seismic hazard potential at the beginning of year 2016. From this point of view, the present work is focused on the imaging of size-scaling distributions such as regional, temporal and magnitude distribution of earthquake activity, completeness magnitude, *Mc*-value, seismotectonic *b*-value and its variations with time, fractal dimension *Dc*-value, precursory seismic quiescence *Z*-value and *GENAS* which estimates the cumulative numbers for different magnitude levels. *ZMAP* analysis software (Wiemer, 2001) was used for all statistical estimations and for all histograms of regional, temporal and magnitude distribution along the VLED fault zone.

2. Geologic and tectonic Structures in and around Albania

The principal geological structures observed in and around Albania are called the Albanides and they form a part of the Dinaric-Albanid-Hellenic arc of the Alpine orogen. The Albanides are located between Hellenides in the south and the Dinarides in the north, which together form the Dinaric branch of the Mediterranean Alpine Belt, limited by the Apulia-Gargano foreland in the west. The Albanides comprise sedimentary and magmatic rocks of Ordovician to Quaternary age (Aliaj et al., 2001). The Albanian orogen and its vicinity are divided into two active tectonic areas (Ormeni et al., 2013): (i) an external compressional field, constituting the Adriatic collision zone (Outer Albanides), and (ii) an internal extensional field (Inner Albanides). In Albania, the Adriatic microplate collides with the Eurasian plate throughout a series of thrusts, with the Albanian orogenic front overthrusting the Adriatic microplate, partially over the Apulian platform and partially over the Albanian Basin (southern Adriatic basin).

The VLED fault zone (Fig. 1), striking north-east, dislocates the structure of the Albanides along their entire width (Sulstarova et al, 1980; Sulstarova et al., 2000). It is expressed by the Vlora and Lushnja flexures, the Dumrea diapire dome, the Elbasani Quaternary depression, the Labinoti transversal structure, and marked by significant Quaternary infill (Melo, 1986). The Golloborda transversal horst continues toward the Tetova Quaternary Graben in FYROM (Sulstarova et al., 2000). From the geological and tectonic point of view, the region is a part of the Krasta tectonic sub-zone, which includes an area of Alpine folding. The Krasta sub-tectonic zone has been deformed by folds, normal faults, and strike-slip faults from movement of the main Alpine orogenic phases (Ormeni et al., 2013). The Okshtuni and Dibra tectonic structures are the north and south parts of the VLED fault zone, respectively. The VLED fault zone shows NE trending nearly 100 km in Albanian region. It is composed of fragmentary normal faults cutting across the Krasta zone and dividing the Mirdita ophiolites zone in two main segments (Aliaj et al., 2001; Ormeni et al., 2013). They represent deep faults that have played an important role in the development and structuring of the Albanides (Sulstarova et al., 2000; for details on geologic, tectonic or neotectonic processes in and around Albania see Ormeni et al., 2013).

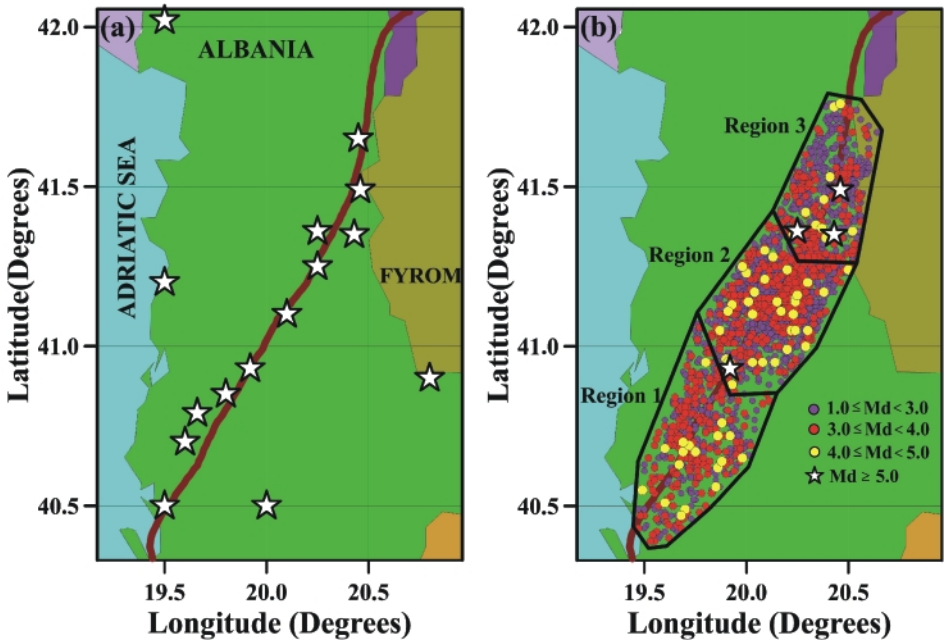

Figure 2: a) Epicenter distributions of earthquakes in and around the VLED fault zone during the 20th century (between 1900 and 2016), b) Seismotectonic subregions and the epicenter distributions of all earthquakes with *MD*≥1.7 and depth<70 km in the VLED fault zone from1967 to 2016. The size of earthquakes is represented by different symbols.

Based on the analysis of the focal mechanisms of moderate and strong earthquakes, the VLED fault zone plays an important role in the seismotectonics of Albania, as well as of the FYROM. The analysis of the focal mechanisms indicates the predominance of normal faulting with a strike-slip component, and NNW-SSE extension in eastern Albania, in response to the convergence between the Adriatic microplate and the Albanian orogen. The VLED fault

zone have produced earthquakes in the past, and they are expected to continue to be active in the future. The studies in the past of moderate and strong earthquakes and their aftershocks have emphasized many geologic and seismotectonic characteristics of this area. As a result, these regions constitute a threat for nearby urban areas of Vlora, Fieri, Berati, Lushnja, Elbasani, Librazhdi, Bulqiza and Dibra towns in Albania, and FYROM.

During the past 95 years, many strong earthquakes occurred in the VLED fault zone. The Elbasani segment has ruptured during earthquake occurred on December 18, 1920, (*M* 5.6), March 31, 1935 (*M* 5.7) and May 19, 2014 (*M* 5.2). The Dibra earthquake of November 30, 1967 (*M* 6.6) is one of the greatest earthquakes that occurred in Albania. The Dibra segment has occurred with the other earthquakes March 30, 1921 Peshkopia (*M* 5.8), August 27, 1942 Peshkopia (*M* 6.0), and September 6, 2009 Gjorica (*M* 5.4). The Lushnja-Fieri section have occurred with September 1, 1959 Lushnja (*M* 6.2), March 18, 1962 Fieri (*M* 6.0), November 16, 1982 Fieri (*M* 5.7) earthquakes. The earthquake that occurred in the Vlora segment was on November 21, 1930 Qaf-Llogaras (*M* 6.0). Strong earthquakes that occurred in recent years in the VLED fault zone can be indicated as May 19, 2014 Cerrik (*M*=5.2) and November 1, 2015 Bulqize (*M*=5.0) earthquakes (Ormeni et al., 2013; Sulstarova and Kociaj, 1975; Sulstarova et al., 1980; 2000). Epicenter distributions of all earthquakes inside of the study region and mentioned above for the 20th century are plotted in Figure 2a.

3. Earthquake Data

The earthquake catalogue used in this study includes a total of 2814 earthquakes which occurred along the VLED fault zone. Magnitude type used for the statistical analyses is duration magnitude, M_D. This catalogue is complete for all magnitude levels and for all time periods between 1967 and 2016. Epicenters of all earthquakes with $1.7 \leq M_D \leq 6.7$ and strong main shocks with $M_D \geq 5.0$ are shown in Figure 2b. Also, a picture of the distribution of the events with different magnitude sizes in Albania and the surrounding region are represented with different symbols in the same figure. Some details for the earthquakes with magnitude $M_D \geq 4.5$ are explained in Table 1. The depths of earthquakes analyzed in this work is limited to shallow earthquakes less than 70 km because these types of seismicity analyses for future seismic hazard, especially in detecting the precursory quiescence anomalies, have provided important outcomes related to the crustal main shocks. In addition to this general approach, the analyses of focal depths reveal that the seismicity in the study region was mainly generated in the shallow upper crust (Ormeni, 2007, 2010).

4. Definition of analysis methods

In this study, statistical analyses of seismic activity are limited to shallow earthquakes with depths less than 70 km because it is generally assumed that the seismogenic layer is about this depth for different parts of the world. As mentioned above, the solutions of focal mechanism in the study region in fact show that earthquake activity is principally produced in the shallow upper crust (Ormeni, 2007, 2010, 2013). Also, some seismicity analyses including the studies of precursory seismic quiescence give significant results for crustal main events in revealing the possible earthquake hazard in a given region. In order to put forth the behaviours of the earthquake activity in the VLED fault zone, a number of statistical

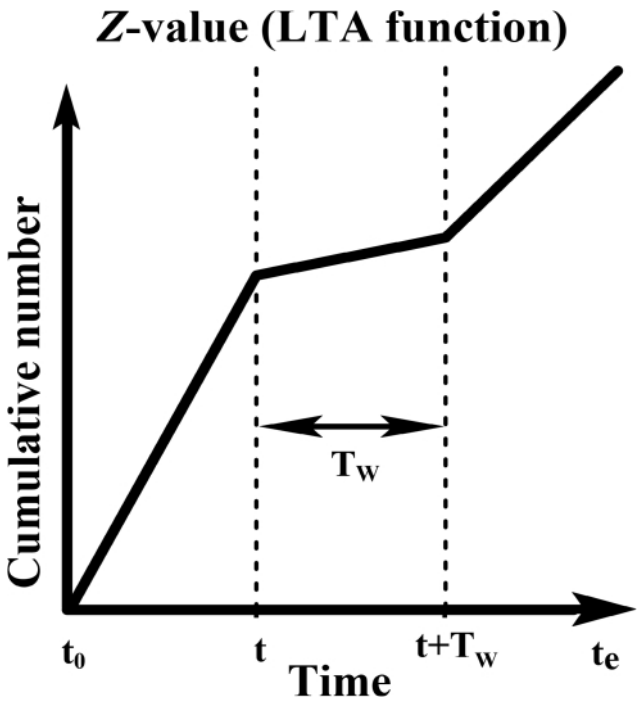

Figure 3: Graphical display of how to calculate *Z*-value. t_o is the beginning time and te is the ending time of the catalogue. The *Z*-value is calculated for all times *t* between t_o and te to T_w and is statistically appropriate for estimating seismicity rate change in a time window T_w in contrast with background seismicity. T_w is the time window length in year and *t* is the current time between t_o and t_e.

Date	Origin Time	Latitude	Longitude	Depth (km)	M_D	Subregion	Place
30/11/1967	7:23:49.00	20.43	41.35	1	6.7	3	Diber
2/12/1967	12:44:41.00	20.20	41.24	1	4.7	2	Elbasan
2/3/1976	19:41:37.00	19.60	40.68	27	4.9	1	Fier
17/3/1989	0:50:51.00	19.98	41.25	1	4.6	2	Kerrabe
6/9/2009	21:49:41.00	20.46	41.49	7	5.4	3	Diber
9/7/2010	22:15:18.00	20.04	41.17	24	4.6	2	Elbasan
19/5/2014	0:59:18.00	19.92	40.93	18	5.2	2	Cerrik
1/11/2015	6:26:17.00	20.25	41.36	2	5.0	3	Bulqize
1/11/2015	6:27 :5.00	20.23	41.35	18	4.8	3	Bulqize

Table 1: Detailed information of earthquakes which occurred in the Vlora-Lushnja-Elbasani-Dibra Transversal Fault Zone with magnitude $4.7 \leq M_D \leq 6.7$ from 1967 to 2015.

parameters are evaluated; histograms of time and magnitude distribution of earthquakes, regional and temporal distributions of seismotectonic *b*-value of Gutenberg-Richter (G-R) relation, fractal dimension *Dc*-value, precursory seismic quiescence *Z*-value, and *GENAS* model.

4.1 Seismotectonic *b*-value (Gutenberg-Richter relation) and importance of Completeness Magnitude, *Mc*-value

A power-law of size distribution of earthquakes is given by Gutenberg and Richter (1944). This empirical relation between frequency of occurrence and magnitude of earthquakes is well described as follows

$$\log_{10}N(M)=a-bM \quad (1)$$

where $N(M)$ is the cumulative number of events with magnitudes larger than or equal to M in a given time period, whereas a and b-values are constants. The a-value changes according to the earthquake activity level; fluctuations in a-value depend on the extend of the study region, time interval of observation, and also the number of earthquakes. The b-value is one of the most important arguments in terms of the seismotectonic properties in a specific area, and it represents the frequency-magnitude distribution of earthquakes. Many studies suggest that the b-value is a scale invariant, and it is related to the distribution of earthquake epicenters and fault segments. A reduction in b-value may result from the decrease in the pressure and an increase of shear stress (Scholz, 1968). Many factors lead to differences of b-values: an increase in thermal gradient, fracture density, material heterogeneity, the number of small and large earthquakes, fault length, stress and strain conditions (Mogi, 1962). The maximum b-value of the frequency-magnitude distribution was estimated by Olsson (1999) and the resulting maximum b-value was given as 1.5 (or with the error limits, between 1.30 and 1.64). However, it is suggested generally that the b-value fluctuates between 0.3 and 2.0 from region to region in different parts of the world (Utsu, 1971).

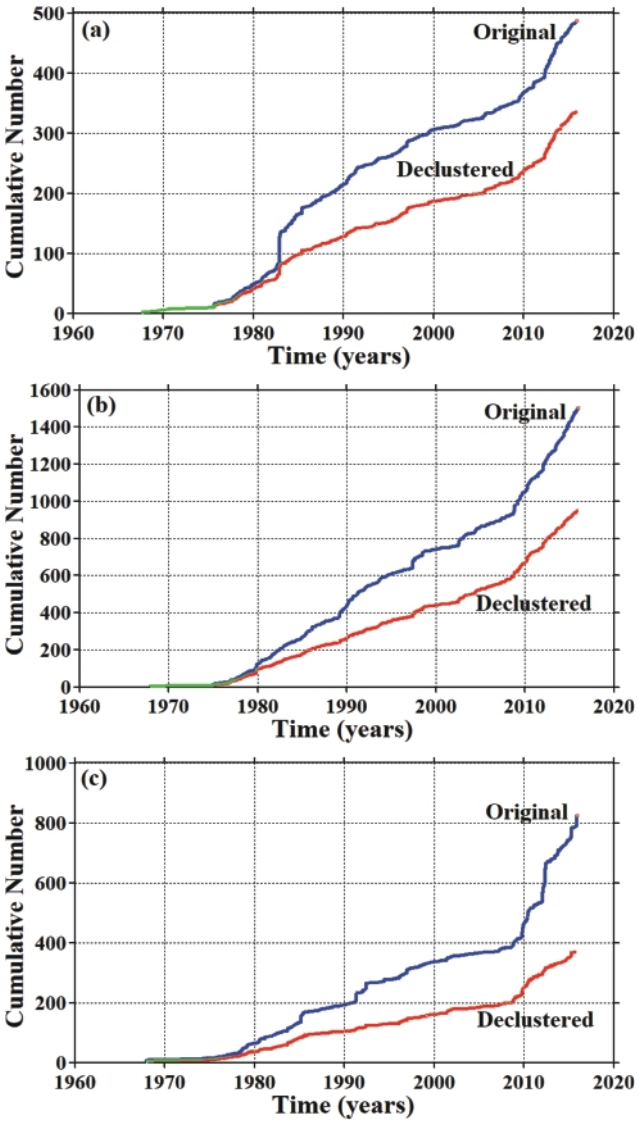

Figure 4: Cumulative number of earthquakes against time for the original and declustered earthquake catalogue for (a): the south western part (region 1), (b): the middle part (region 2), and (c): the north eastern part (region 3) of the VLED fault zone.

The selection of the regression model which is used in the estimation of the b-value is a sensitive and significant point. Although there are a number of methods to calculate the b-value, the best known and commonly used is the maximum likelihood model by Aki (1965). The b-value was generally determined graphically, but a more effective analysis is performed using the maximum likelihood method. It was derived from the quality of the first order moment, and later Aki (1965) showed that the maximum likelihood estimate maximizes the likelihood function. As a result, the b-value can be written as follow:

$$b = \frac{2.303}{(M_{mean}-M_{min}+0.05)} \quad (2)$$

where M_{mean} is the mean magnitude of the events, and M_{min} is the minimum magnitude in the catalogue. The coefficient of 0.05 is a correction constant. Local changes in M_{min} can be estimated correctly if relatively large numbers (100 or so) of local measurements are available for analysis. Confidence limits of 95 % on the estimations of b-value are $\pm 1.96\ b/\sqrt{n}$, where n is the number of earthquakes. This estimate gives the confidence limits of ±0.1-0.2 regarding the b-value for a characteristic sample of n=100 events. As a result, the number of earthquakes in this study is 487 for region 1, 1503 for region 2, and 824 for region 3. The value of n=100 earthquakes is an ordinary example for estimations and it represents a specific calculation.

In many studies related to the frequency-magnitude distribution and precursory seismic quiescence, the usage of the maximum number of earthquakes is very important for reliable results. For this reason, the estimate of completeness magnitude, *Mc*-value, is one of the most significant process. *Mc*-value can be described as the minimum magnitude of

complete reporting. In other words, the completeness magnitude is that magnitude above which all earthquakes which occur are reported (Habermann, 1983). It means that this magnitude level includes 90% of the earthquake data which can be sampled with a power law fit (Wiemer and Wyss, 2000). *Mc*-values show regional and temporal changes in different networks and catalogues. It is well known that the *Mc*-value shows a decrease with time since the number of seismographs increases and the techniques for *Mc* estimation improve. Small events may not be recorded since they fall within the coda of larger earthquakes and so, *Mc*-value will be larger in the early part of the catalogue. If large *Mc*-values are excluded from the catalogue, the minimum magnitude level can be lowered and the number of the earthquakes available for analyses can be increased. For the seismicity studies which depend on complete sets of small earthquakes, the minimum magnitude level in the calculations should be raised to the highest *Mc*-value. Temporal variations of *Mc*-value can be calculated rapidly and safely by evaluating the goodness of fit to a power law.

The assumption of Gutenberg Richter's power-law distribution against magnitude can be used to calculate the *Mc*-value. The variations of *Mc*-value as a function of time is provided by using a moving time window approach with the maximum likelihood method (for details see Wiemer and Wyss, 2000). Since the *Mc*-value will be larger in the early part of the catalogue, temporal variations in this parameter may produce wrong seismicity estimations, particularly in *b*-value. Variations in the *Mc*-value depend on the earthquake activity of the study region and the sensitivity of the stations. Consequently, the investigation of the precursory seismic quiescence and estimation of the *b*-value are affected from the choice of *Mc*-value. For the temporal changes of the magnitude-frequency distribution of earthquakes and for the regional variability of seismic quiescence, the knowledge of temporal changes in *Mc*-values is necessary. As an important precondition, the estimations of the *Mc*-value for different parts of the VLED fault zone are made with great care since this type of completeness analysis has a great importance for all statistical calculations in this study.

4.2 Fractal dimension (Correlation Dimension, *Dc*-value)

Fractal dimension is a real number and measures the geometry of a distribution and most likely changes with space and time. Fractal studies are commonly preferred to analyze the clustering properties and size-scaling characteristics of earthquake parameters, assuming that earthquake distributions are fractal. Fractal studies define the self-similarity of a geometrical object. A further generalization leads to the correlation dimension *Dc* which is not based on a covering of the regarded set, but on the distances between pairs of points of the set (Goltz, 1998). Fractal distributions are the only distributions which do not include a typical length scale, and so, can be practicable to scale invariant phenomena. Grassberger and Procaccia (1983) presented an analysis model based on the distances between pairs of points. This correlation dimension was called sphere counting and is among the most widely used. Using the two-point correlation dimension *Dc*, Grassberger and Procaccia (1983) defined the correlation dimension *Dc* and the correlation sum *C*(*r*) as follows:

$$Dc=\lim_{r\to 0}[\log C(r)/\log r] \quad (3)$$

$$C(r)=2N_{R<r}/N(N\text{-}1) \quad (4)$$

where *C*(*r*) is the correlation function, *r* is the distance between two epicenters and *N* is the number of earthquakes pairs separated by a distance *R*<*r*. If the epicenter distributions of events have a fractal structure, the next equation can be defined as follows:

$$C(r)\sim r^{Dc} \quad (5)$$

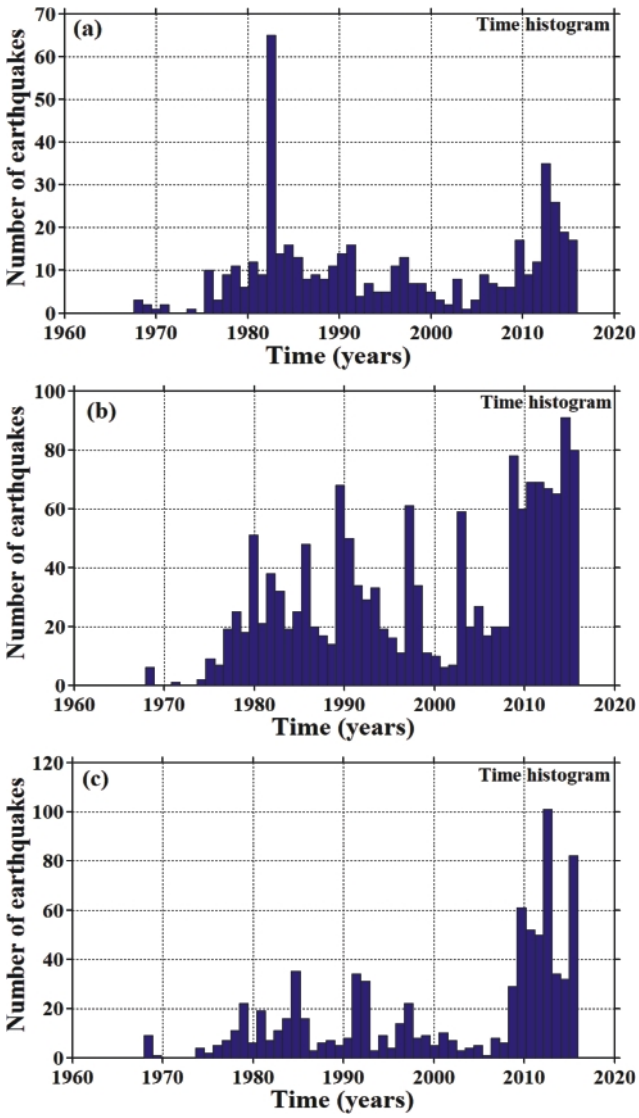

Figure 5: Time histograms of the earthquake distributions for: (a) the south western part (region 1), (b): the middle part (region 2), and (c): the north eastern part (region 3) of the VLED fault zone.

where *Dc* is a fractal dimension, more generally, the correlation dimension. The distance *r* (in degrees) between two earthquakes can be computed from:

$$r=\cos^{-1}(\cos\theta_i \cos\theta_j+\sin\theta_i \sin\theta_j \cos(\Phi_i-\Phi_j)) \quad (6)$$

where (θ_i,Φ_i) are the latitudes of i^{th} events and (θ_j,Φ_j) are the longitudes of the jth events (Hirata, 1989). Fractal dimension is described by fitting a straight line to a plot of log *C*(*r*) against log r. *C*(*r*) is not affected by the lack of points outside the cluster if r is small. Therefore, *C*(*r*) increases quickly with r, and the *Dc*-value will be large. Hence, strong clustering would correspond to an increase in *Dc*-value if a scaling range using small values of r is used to estimate *Dc*-value. The rate at which *C*(*r*) rises with r decreases, and *Dc*-value will be small when r comes close to the diameter of the cluster. If a scaling range using high values of r is used to estimate the *Dc*-value, strong clustering would correspond to a decrease in *r*. Depending on the range of r chosen, this means that a dense cluster of points can yield both great and small *Dc*-values. In practice, fractal systems in nature are self-similar over a finite range, so *Dc*-value must be estimated from a range which is not sensitive to the finiteness of the set.

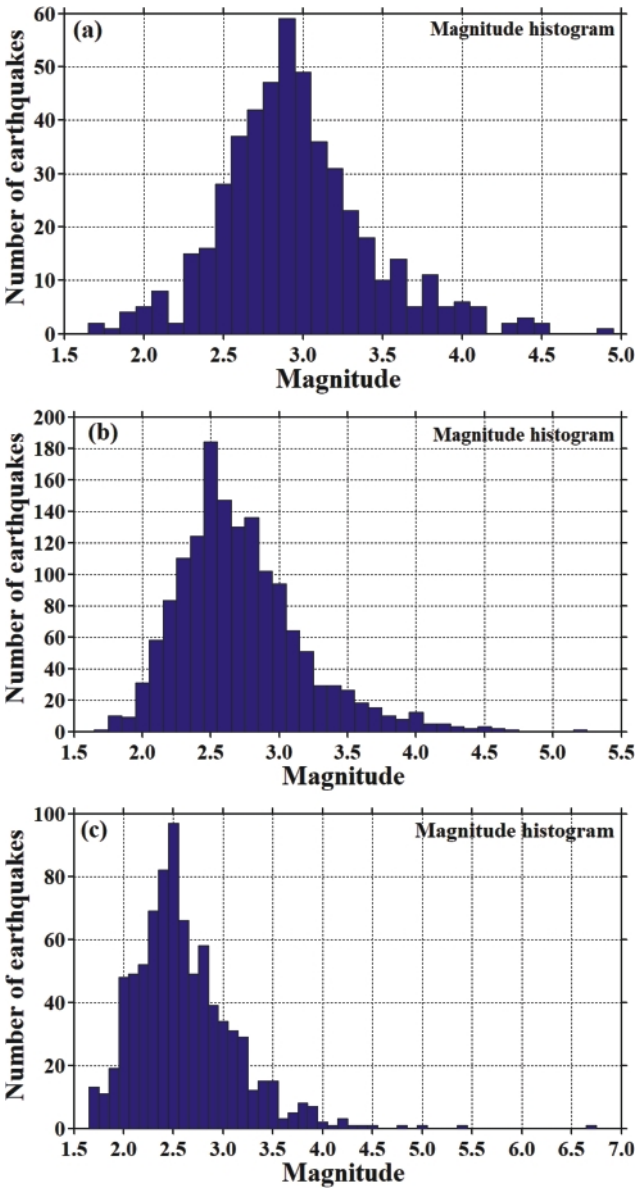

Figure 6: Histograms of MD magnitudes of the earthquake distributions for: (a) the south western part (region 1), (b): the middle part (region 2), and (c): the north eastern part (region 3) of the VLED fault zone.

The nature of spatial and temporal fractal characteristics of the events is qualified by fractal, especially by the correlation dimension (Kagan, 2007). Distributions of earthquakes comply with the fractal statistics and so, earthquakes can be qualified by fractal dimension. Fractal dimension may be estimated in order to avoid the probable unbroken fields, and these unbroken areas are proposed as potential seismic gaps to be broken next (Toksöz et al., 1979). This means that changes in fractal characteristics are mainly related to the complexity or quantitative measure of the heterogeneity degree of the earthquake activity on the fault system. Smaller *b*-value which is related to larger *Dc*-value is the dominant characteristic in the field of increased complexity for an active fault regime. As an important result, this may arise from the clusters of earthquakes, and the variations in *Dc*-value may provide some evidences for evaluations of stress relaxation on the fault regions (Öncel and Wilson, 2002; Polat et al., 2008).

4.3 Process for declustering of earthquake data and standard normal deviate *Z*-test (Precursory Seismic Quiescence, *Z*-value)

Foreshocks, aftershocks or earthquake swarms usually mask the temporal distribution of the number of events. Hence, these types of complex data sets affect the results of analyses on earthquake statistics. In order to make a quantitative rate change analysis of earthquake activity, all dependent events must be eliminated from the catalogue. In order to separate the dependent events from independent ones, the earthquake catalogue is declustered by using the Reasenberg (1985) algorithm. Arabasz and Hill (1996) stated that cluster procedure "declusters" or decomposes an earthquake catalogue into main and secondary events. With the usage of a declustering process, all dependent earthquakes can be extracted from each cluster, and they can be represented by a single event. This elimination process is a significant stage for reliable and high quality results of these types of quiescence assessments. In order to decluster the earthquake catalogue used in this study, Reasenberg (1985) algorithm within the *ZMAP* software (Wiemer, 2001) is used, and precursory quiescence analysis is made by using the resulting declustered data. After Wiemer (2001), many authors have used *ZMAP* software for the analysis of seismic quiescence in different parts of the world (e.g., Katsumata and Kasahara, 1999; Chouliaras and Stavrakakis, 2000; Polat et al., 2008; Öztürk, 2011; 2013; 2015; Öztürk and Bayrak, 2012; Ali, 2016).

We declustered the earthquake catalogue by using the algorithm given by Reasenberg (1985). It is well known that

	Region 1	Region 2	Region 3
Study area	40.3-41.1°N, 19.2-20.2°E	40.8-41.4°N, 19.8-20.6°E	41.2-41.8°N, 20.1-20.6°E
Time period	20 July 1967 9 December 2015	12 December 1967 26 December 2015	30 November 1967 15 December 2015
Time length (decimal year)	48.39	48.07	48.04
Completeness magnitude (Mc)	2.7	2.5	2.5
Depth interval (km)	1-70	1-60	1-60
Number of earthquakes(original catalogue)	487	1503	824
Number of earthquakes (declustered catalogue)	337	953	370
Grid space	0.01°x0.01°	0.01°x0.01°	0.01°x0.01°
Nearest earthquakes (N)	40	40	40
Time window (year)	5.5	5.5	5.5
Time steps (day)	28	28	28

Table 2: Some details of the original and declustered catalogue for different parts of Vlora-Lushnja-Elbasani-Dibra Transversal Fault zone. The other input parameters used in the statistical analyses are also given.

the declustering process introduces some artificial manipulations. Actually, the declustering process contains some optional parameters which allow the user to eliminate the dependent events in a smaller or larger time or space interval with respect to location of the main event (for details see Arabasz and Hill, 1996). The study region is divided into three parts (Fig. 2b): the south western part (region 1), middle part (region 2) and the north eastern part (region 3) of the VLED fault zone. The original catalogue consists of 2814 earthquakes between July 20, 1967 and December 26, 2015, a time period of about 48.5 years. After the selection of different regions, earthquake catalogues in these areas are arranged for the analyses. Time variations of completeness magnitude for different parts of the VLED fault zone will be explained below (see Fig. 7).

There are 487 earthquakes with $M_D \geq 1.7$ in region 1 (south western part) of the VLED fault zone. The declustering process eliminates 47 events and 440 earthquakes are obtained. Thus, this algorithm took away about 9.65 % of earthquakes from all data set. The *Mc*-value is calculated as 2.7 for this region and the events with magnitudes smaller than 2.7 are removed from the declustered catalogue. The number of events exceeding this completeness magnitude level is 103. These two processes excluded 150 earthquakes and, in total, 30.8 % of the earthquakes are removed from the whole catalogue of region 1. The earthquake catalogue for quiescence analysis includes 337 earthquakes in the south western part of VLED fault zone.

There are 1503 events with $M_D \geq 1.7$ in region 2 (middle part) of the VLED fault zone. The declustering procedure removes 178 earthquakes and results in 1325 events. Thus, this algorithm took away about 11.84 % of events. The *Mc*-value is found as 2.5 for region 2 and earthquakes with $M_D < 2.5$ are excluded from the declustered catalogue. The number of earthquakes exceeding this completeness magnitude level is 372. These two procedures removed 550 events and 36.66 % of the events in total are taken away from the whole catalogue of region 2. Consequently, the earthquake catalogue for quiescence assessment consists of 953 events in the middle part of VLED fault zone.

In region 3 (north eastern part) of the VLED fault zone 824 events with $M_D \geq 1.7$ are recorded. The declustering procedure

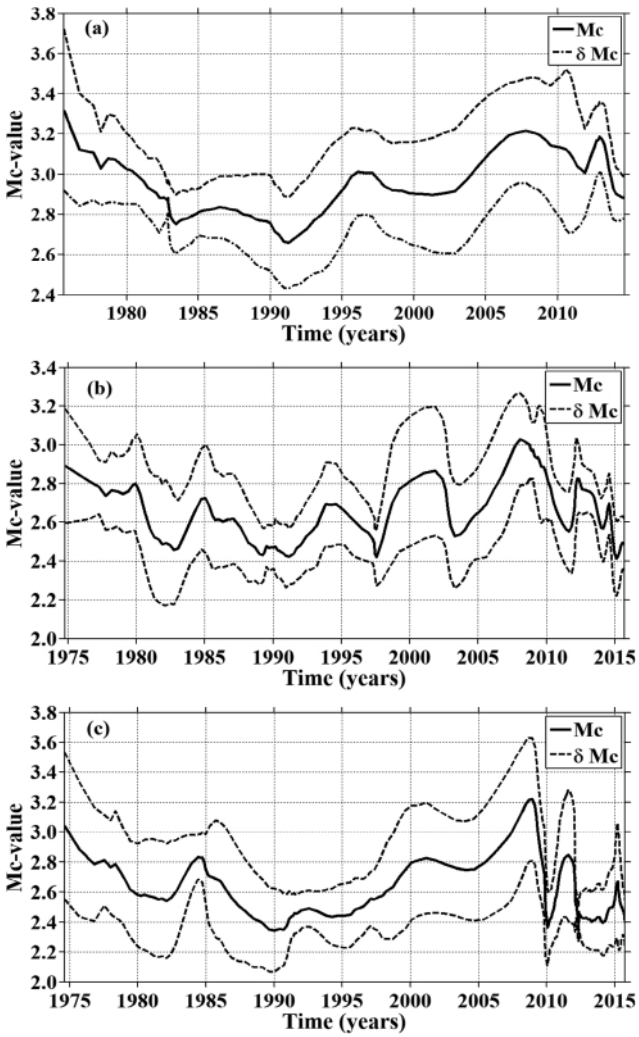

Figure 7: Changes in magnitude completeness, *Mc*, with time for: (a) the south western part (region 1), (b): the middle part (region 2), and (c): the north eastern part (region 3) of the VLED fault zone. Standard deviation, δMc of the changes (dashed lines) are also shown. *Mc*-values are estimated for overlapping samples, each including 400 events for all parts of the VLED fault zone.

removes 226 earthquakes and 598 earthquakes are obtained. Thus, this algorithm removes about 27.4 % of earthquakes from whole data set. The *Mc*-value is estimated as 2.5 for region 3 and the events with M_D<2.5 are subtracted from the declustered catalogue. The number of events exceeding this completeness magnitude level is 228, removing 454 events and 55.1 % of the events in total. As a result, the earthquake catalogue for quiescence evaluation includes 370 earthquakes in the north eastern part of VLED fault zone. An extract of some parameters for the original and declustered earthquake catalogue is given in Table 2.

Precursory seismic quiescence analysis can be achieved by the methodology provided in Wiemer and Wyss (1994) and performed in *ZMAP* software. Although there are a number of techniques which identify the earthquake rate changes, many of these methods have used the precursory quiescence phenomenon. The best known and the most commonly used of these techniques are the standard normal deviate *Z*-test (for details see Wiemer and Wyss, 1994). *ZMAP* software has been used by many researchers in order to analyze the seismicity rate changes for different parts of the world, only a brief description will be given here. *ZMAP* technique allows to users to analyze and to produce graphic displays of seismicity rate changes. In this study, the *ZMAP* method is used to put forth the areas exhibiting anomalous regions of quiescence. In order to rank the importance of quiescence, standard normal deviate *Z*-test is used, generating Log Term Average, LTA (*t*), function for the statistical assessment of the confidence level in units of standard deviations:

$$Z(t)=\frac{R_{all}-R_{wi}}{\sqrt{\frac{\sigma^2_{all}}{n_{all}}+\frac{\sigma^2_{wi}}{n_{wi}}}} \quad (7)$$

where R_{all} is the mean earthquake rate in the overall period including T_w (from t_0 to t_e), R_{wi} is the average earthquake rate in the considered time window (from t to $t+T_w$), σ and n are the standard deviations and the number of samples within and outside the window; t is the current time ($t_0 < t < t_e$). The *Z*-value is calculated by the equation for all times t between t_0 and t_e to T_w (Fig. 3). The Z-value is estimated as a function of time, letting the foreground window slide along the time period of catalogue, called LTA (*t*).

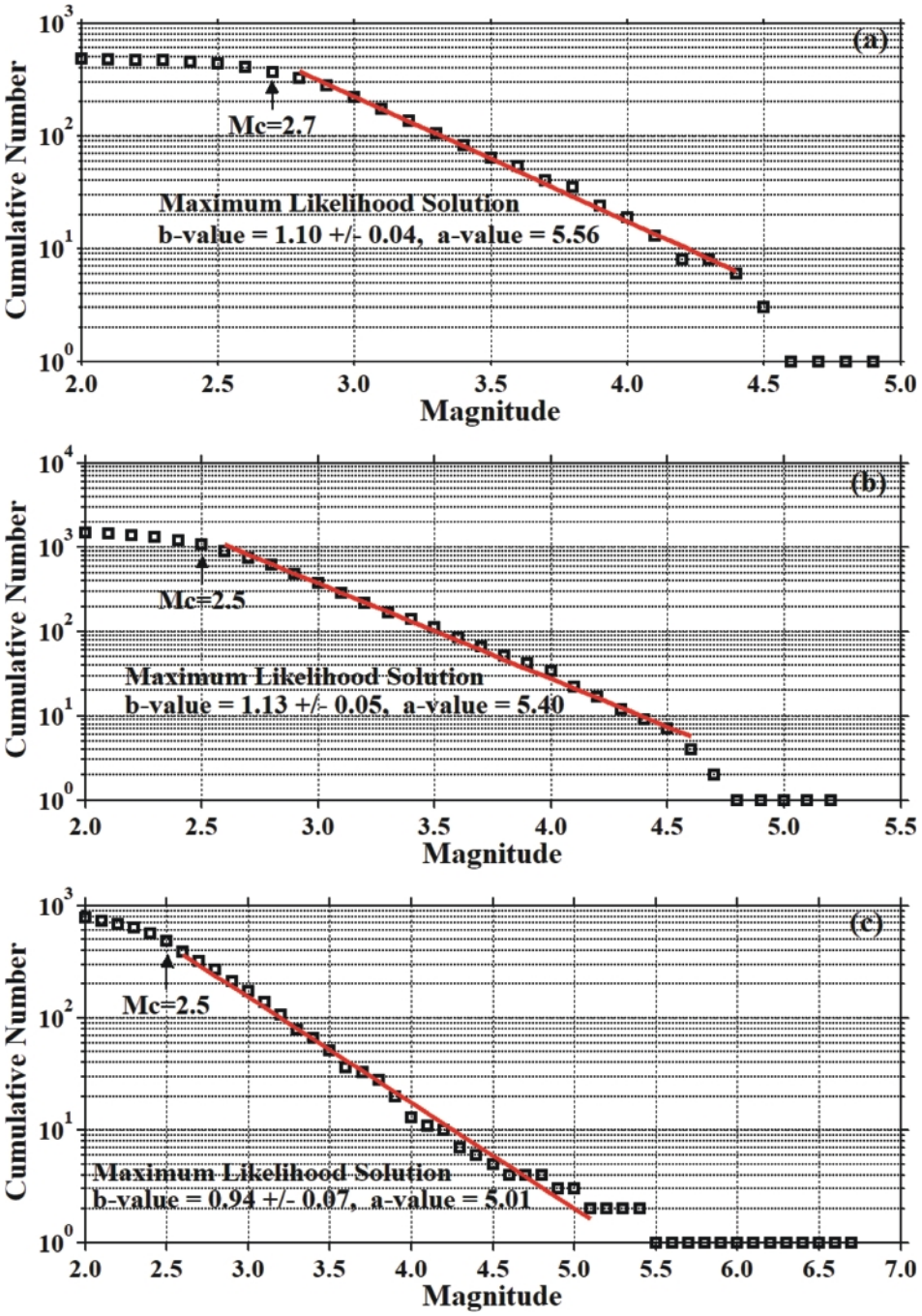

Figure 8: Gutenberg-Richter relations of all events between 1967 and 2016 for: (a) the south western part (region 1), (b): the middle part (region 2), and (c): the north eastern part (region 3) of the VLED fault zone. The *b*-value and its standard deviation, the *Mc*-value and *a*-value in the magnitude-frequency distribution are also given.

5. Results of statistical investigations of recent seismicity and discussions

A statistical evaluation of the recent earthquake activity in the Vlora-Lushnja-Elbasani-Dibra

transversal fault zone in Albania is achieved with the analysis of the seismotectonic *b*-value, fractal dimension *Dc*-value, standard normal deviate *Z*-value, and also by mapping the regional, temporal and magnitude histograms between 1967 and 2016. The *b*-value of magnitude-frequency relation supplies a relative assessment of the likelihood for small and large magnitudes of earthquakes. The relation between fractal dimension and earthquake activity describes the complex features and patterns of earthquake occurrences. Estimates of the standard normal deviate *Z*-value provide valuable information in detecting the precursory seismic quiescence anomalies for crustal main shocks, and it also can supply additional perspective to future seismic hazard for a given region. Thus, we focused on estimating these types of parameters and interpretation of the relationships among them in terms of the next earthquake potential.

Figure 4 shows the cumulative number of earthquakes against time in all parts of the VLED fault zone both for the original and declustered earthquake catalogue. As seen in Figures 4a-4c, any significant changes are not reported in seismicity from 1967 to 1976. A slight change is observed in the earthquake activity between 1976 and 1983 for region 1, between 1976 and 1980 for regions 2 and 3. However, the number of earthquakes gradually increases after 1983 for region 1, after 1980 for regions 2 and 3. Also, significant fluctuations in the earthquake activity are reported in all regions, especially after the 2000s. As shown in Figure 4, the cumulative number of declustered catalogues with larger than or equal to completeness magnitude as a function of time has a smoother slope than that of original catalogues. As an important result, we can clearly state that declustering process has eliminated dependent earthquakes from the original earthquake catalogue and this process has provided a more reliable, robust and homogeneous earthquake catalogue.

Time histograms for the three regions (Fig. 5a) show the maximum increase in the number of events in 1983 for region 1, and a slight increase after 2012. The histogram for region 2 (Fig. 5b) indicates that there are increases in the number of earthquakes in 1980, 1986, 1990, 1998, 2003, and after 2008 and 2013. The time histogram for region 3 (Fig. 5c) shows a small increase between 1980 and 2010, and a prominent increase in the number of events after 2010.

In addition to the time histograms, we mapped the magnitude histograms for all parts of the VLED zone. The M_D magnitudes of earthquakes in these three regions change between 1.7 and 6.7, and earthquake numbers show an exponential decay rate from the smaller to larger magnitudes. A lot of the earthquakes are between 2.5 and 3.5 levels for region 1, and between 2.0 and 3.0 levels for regions 2 and 3 (Fig. 6). There is a maximum magnitude at M_D=2.9 in region 1 (Fig. 6a), at M_D=2.5 in regions 2 (Fig. 6b) and 3 (Fig. 6c).

As mentioned above, the changes in *Mc*-value are quite effective on the analysis of precursory seismic quiescence and the Gutenberg-Richter *b*-value. For this reason, the analyses of completeness magnitude as a function of time is achieved by a moving window technique with the maximum curvature method (Woessner and Wiemer, 2005). The *Mc*-value is calculated for samples of 40 earthquakes per window for region 1 with the catalogue consisting of all 487 earthquakes of $M_D \geq 1.7$, 40 events per window for region 2 with the catalogue including all 1503 earthquakes of $M_D \geq 1.7$, and 40 events per window for region 3 with the catalogue having 824 earthquakes of $M_D \geq 1.7$. The *Mc*-value is relatively large, and changes between 2.8 and 3.3 from 1967 to 1983 (Fig. 7a), whereas it fluctuates around 2.8 between 1983 and 1995. After 1995, the *Mc*-value is between 2.9 and 3.2 for region 1. The *Mc*-value is around 2.8 until 1980 while it changes between 2.4 and 2.8 from 1980 to 2000 (Fig. 7b), and fluctuates between 2.5 and 3.0 from 2000 to 2010, and then these large values decrease from 2.8 to 2.4 between 2010 and 2016. For region 3, *Mc*-value changes between 2.6 and 3.0 from 1967 to 1985 and, be-

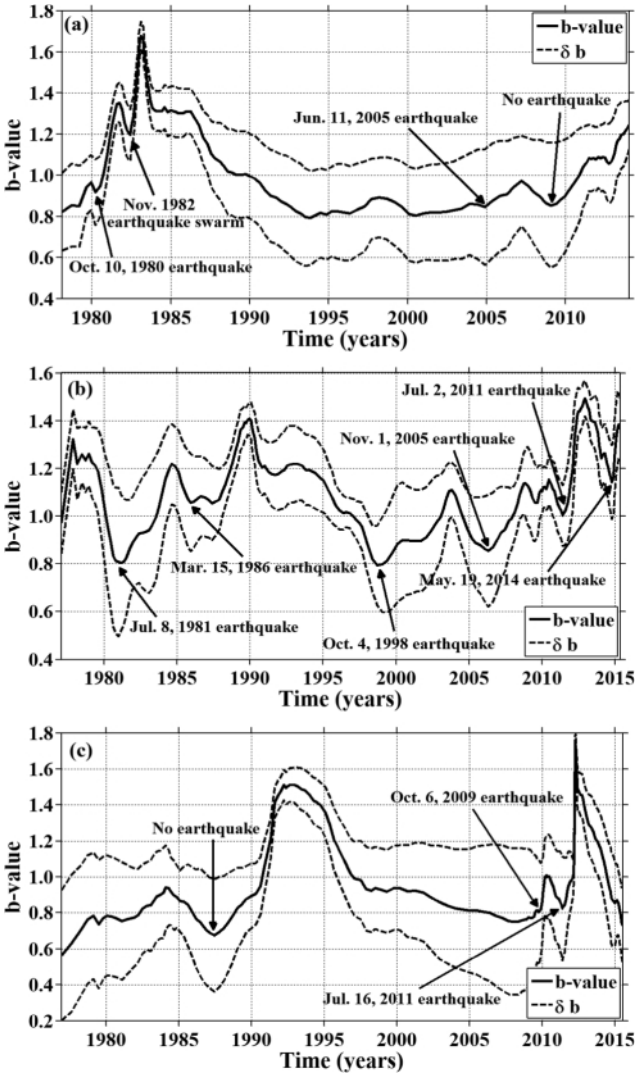

Figure 9: Changes in *b*-values with time for: (a) the south western part (region 1), (b): the middle part (region 2), and (c): the north eastern part (region 3) of the VLED fault zone. The *b*-values were computed for overlapping examples of 75 events for regions 1 and 3, 100 events for regions 2. Standard deviation (δb) of the *b*-values (dashed lines) is also given. Arrows show the great decrease in *b*-values before the occurrences of strong earthquakes in the regions.

tween 2.8 and 2.4 from 1985 to 2005 (Fig. 7c). In region 3, there are some fluctuations in *Mc*-value from 3.2 to 2.4 after 2005. This high value is around 2.6 between 2010 and 2016. It is well known that *Mc*-value is not stable as a function of time and is a very important parameter for these types of statistical analyses. As a significant result, we clearly saw that an average of *Mc*=2.7 for region 1, and *Mc*=2.5 for regions 2 and 3 well represent the data for all statistical evaluations of different parts of the VLED fault zone.

It is well known that the maximum likelihood method gives a more powerful estimation than the least-square curve fitting method (Aki, 1965). Hence, we used this method to estimate the *b*-value of G-R relation for all parts of the VLED fault zone. Awad et al. (2005) stated that the G-R power law characterizes the statistical properties of seismic source zones in energy domain using the magnitude-frequency distribution of earthquakes.

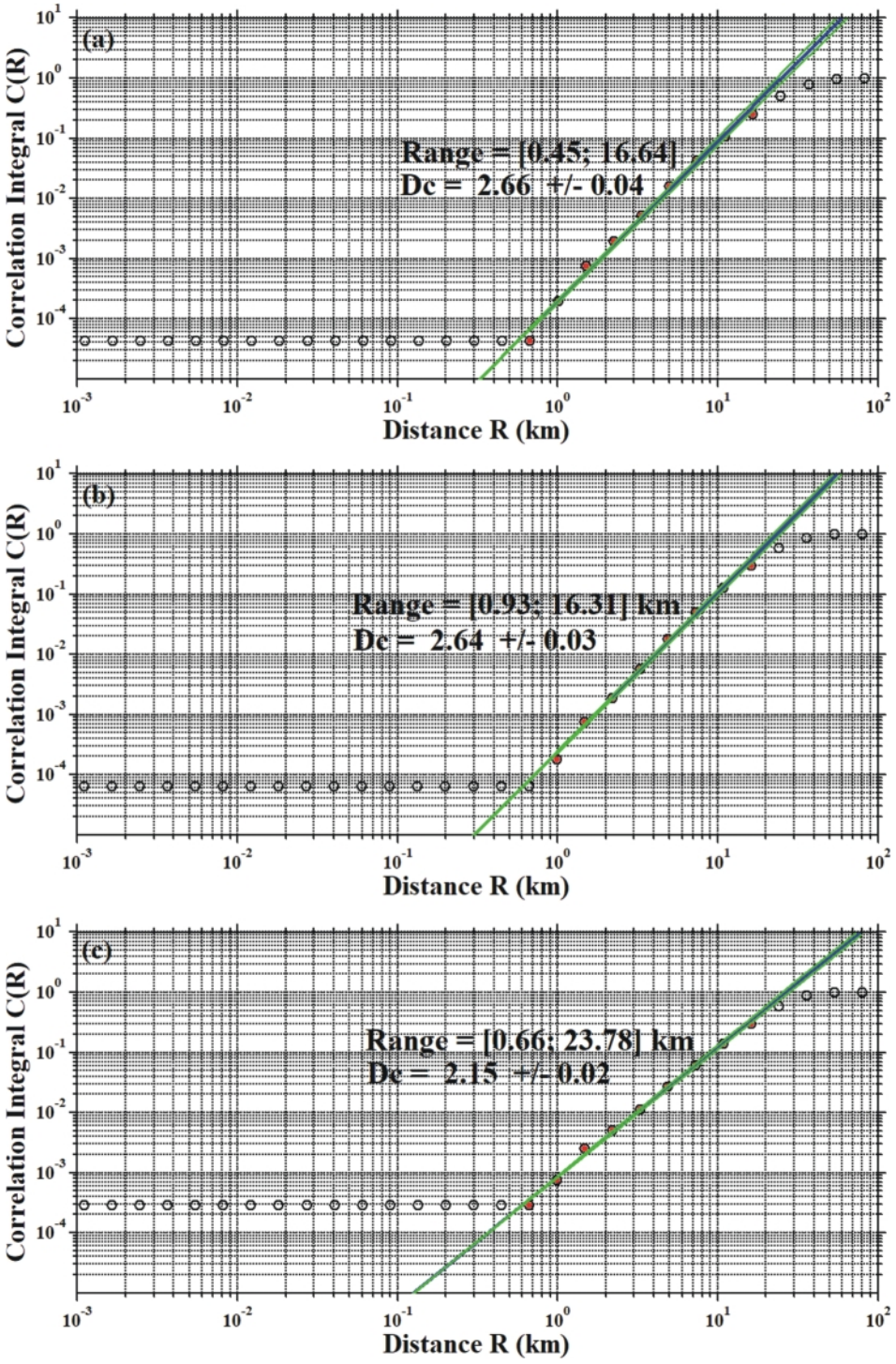

Figure 10: Fractal dimension *Dc*-values for: (a) the south western part (region 1), (b): the middle part (region 2), and (c): the north eastern part (region 3) of the VLED fault zone. The slope of the black lines gives the Dc-values. Standard deviations of the *Dc*-values are also given in dashed lines.

Cumulative numbers of earthquakes versus magnitude for different parts of the study region are shown in Figure 8. For the south western part (region 1) of the VLED fault zone, *b*-value is estimated as 1.10±0.04 with *Mc*=2.7 (Fig. 8a) using all 487 earthquakes ($M_D \geq 1.7$ and depth <70 km). The *b*-value is calculated as 1.13±0.05 with *Mc*=2.5 using all 1503 events ($M_D \geq 1.7$ and depth<70 km) for the middle part (region 2, Fig. 8b) of the VLED fault zone. The *b*-value is found as 0.94±0.07 with *Mc*= 2.5 (Fig. 8c) using all 824 earthquakes ($M_D \geq 1.7$ and depth<70 km) for the north eastern part (region 3) of the VLED fault zone. As shown in Figure 8, the *b*-value, its standard deviation, *a*-value and *Mc*-value are given. An average *b*-value is assumed as approximately equal to 1.0 (Frohlich and Davis, 1993) and tectonic earthquakes are represented with a b-value between 0.5 and 1.5. However, the *b*-value for region 3 is smaller than the average *b*-value of 1.0 and consequently, this lower *b*-value may indicate an increase of shear stress in the north eastern part of the VLED fault zone in the recent years. As a clear result, we can say that frequency-magnitude distributions of earthquake catalogues for all regions are well described with the G-R power law having a characteristic *b*-value close to 1.0.

Temporal changes of the *b*-values for different parts of the VLED fault zone are given in Figure 9. The variations in *b*-values

are examples for the size of 75 events for regions 1 and 3, and 100 events for region 2. There are clear decreases in *b*-value smaller than 1.0 before some strong main shocks such as October 10, 1980 and June 11, 2005 earthquakes (Fig. 9a), while some declines in *b*-value are not related to the occurrence of a main shock. A remarkable result is that there exists an earthquake swarm in November 1982 and a significant increase is observed in the *b*-values with a maximum of *b*~1.35 until this date. After this, a clear decrease is observed around *b*~1.2 before the beginning of earthquake swarm. This also means that earthquake swarms have a larger *b*-value than other earthquake occurrences. These types of increases and decreases in *b*-values are also detected before some strong earthquake occurrences in regions 2 and 3. In the middle part of the VLED fault zone, we observed many systematic decreases before the occurrences of some main shocks such as July 8, 1981, March 15, 1986, October 4, 1998, November 1, 2005, July 2, 2011, and May 19, 2014 earthquakes (Fig. 9b). For region 3, there are regular decreases around *b*~0.8 before the occurrences of two main shocks, October 6, 2009 and July 16, 2011 earthquakes while any strong earthquake is not observed after a decrease in *b*-value in 1987 (Fig. 9c). A significant observation from Figure 9c is that a clear systematic decrease started after 2012 and it continues at the beginning of 2016.

As stated in Utsu (1971), many factors can affect the changes in *b*-value. The *b*-value for a region does not reflect only the relative proportion of the number of large and small events, but is also related to the stress situation in the region. Temporal changes of *b*-values are one of the most important precursors for earthquake occurrences. The changes in *b*-value as a function of time show a tendency to decrease before the occurrence of large earthquakes (Öztürk, 2011; Prasad and Singh, 2015; Wang et al., 2016). Öztürk (2011) observed large decreases before the occurrences of several large earthquakes in Turkey such as August 17, 1999 İzmit, November 12, 1999 Düzce, January 27, 2003 Tunceli, and May 1, 2003 Bingöl earthquakes. Prasad and Singh (2015) observed a correlation between low *b*-value for the one-year time interval and the occurrence of large main shocks. They suggested that changes in *b*-value can be used to forecast a major earthquake. Wang et al. (2016) stated that seismic observations show abnormal *b*-value changes before the occurrence of some main shocks. We can point out that the decreasing trend in *b*-value before the occurrences of some strong main shocks may result from a stress increase. The systematic decreasing trend in *b*-value starts in 2012 and continues in 2015 for region 3. As a very remarkable result, these changes are very important for earthquake forecasting, and we can interpret that these fluctuations can be an indicator of next earthquake in the north eastern part of the VLED fault zone (region 3).

The correlation dimension *Dc*-value of earthquake epicenter distribution in different parts of the VLED fault zone is calculated by fitting a straight line to the curve of the correlation integral, *C*(*R*), versus the distance, *R*. *Dc*-values for three parts of the study region are estimated with 95% confidence limits by linear regression fit (Fig. 10). The *Dc*-value is computed as 2.66±0.04 for the distribution of 487 events in the south western part of the VLED fault zone (region 1, see Fig. 10a). Using the distribution of 1503 earthquakes in the middle part of the study region (region 2), the *Dc*-value is calculated as 2.64±0.03 (Fig. 10b). The *Dc*-value is estimated as 2.15±0.02 (Fig. 10c) for the distribution of 824 events in the north eastern part of the VLED fault zone (region 3). There are a clear linear range and scale invariance in the fractal statistics between 0.45 and 16.64 km for the south western region 1 (Fig. 10a), between 0.93 and 16.31 km for the middle part (Fig. 10b), between 0.66 and 23.78 km for the north eastern part (Fig. 10c) of the study region. *Dc*-values and their standard deviations are also estimated within these distances.

As mentioned above, the fractal dimension may define the earthquake distributions since they match the fractal statistics. It is well known that the higher *Dc*-values are related to active faults and these fault systems have an increasing complexity (Öncel and Wilson, 2002). Also, the faults in which earthquakes are caused by failure of isolated, small asperities and occurred in clusters have lower *Dc*-values (Barton et al., 1999). Öztürk (2015) stated that the higher order correlation dimension, especially larger than 2.3 is increasingly sensitive

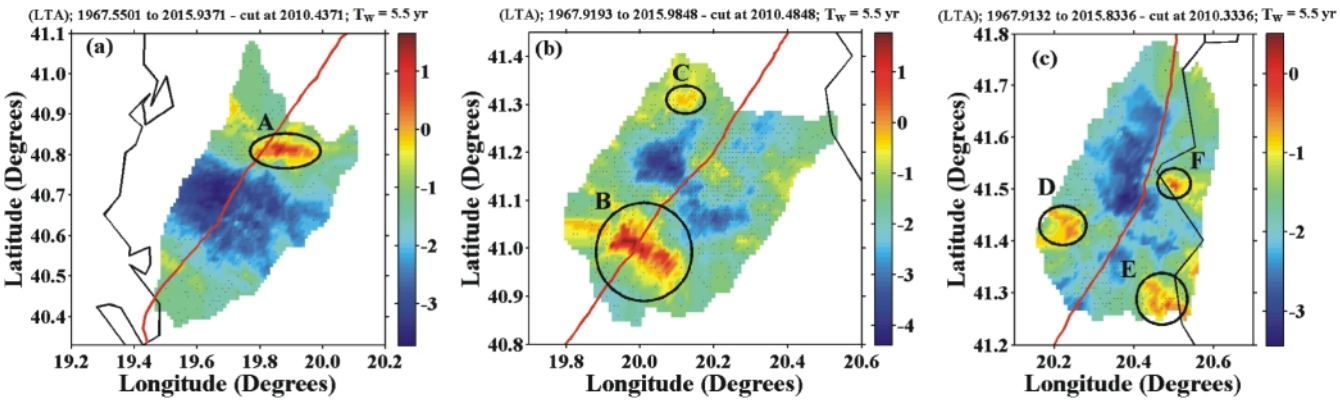

Figure 11: Changes in *Z*-values in the beginning of 2016 with T_W=5.5 years for: (a) the south western part (region 1), (b): the middle part (region 2), and (c): the north eastern part (region 3) of the VLED fault zone. Black dots show the declustered events with $M_D \geq 2.7$ for region 1, $M_D \geq 2.5$ for regions 2 and 3.

to the heterogeneity in magnitude distribution. This means that earthquake activity is more clustered in smaller areas (or at larger scales) in the south western and the middle parts of the VLED fault zone. As a remarkable conclusion, we can generally assume that the higher *Dc*-values are the dominant structural properties in the VLED fault zone and may result from the earthquake clusters. Because the uniform distribution of events decreases with an increase in the earthquake clustering, this large values can also be an indication of variations in the stress distribution in the study area.

Regional variations of standard normal deviate *Z*-value in different parts of VLED fault zone are mapped at the beginning of 2016 (Fig. 11). Each Z-value has a different interpretation: the lowest Z-values mean that the changes in earthquake activity are not significant, and the largest *Z*-values indicate a decrease in seismicity rate. To image the regional changes of precursory seismic quiescence, declustered earthquake catalogues for all regions are used. For all three parts, we used regional grid of points with a grid of 0.01°. After several tests for all regions, the nearest events *N*=40 are selected at each node and the changes of earthquake activity are mapped with the maximum radius changes by a moving time window T_w (or sometimes *wl*) as stated in Wiemer and Wyss (1994). An important point in this stage is that statistical robustness of the LTA (*t*) function increases with the size of T_w and so, more and more smooth shape is obtained if the length of T_w exceeds the anomaly period. For this reason, we made a few tests by trying different T_w-values such as 1.5, 2.5, 3.5, 4.5, and 5.5 years. Thus, we decided that quiescence anomalies are better visible for the length of time window T_w=5.5 years and we used this T_w=5.5 value for the imaging of regional changes of earthquake activity rate. Finally, we separated the event population into many groups with the span of 28 days for all regions in order to obtain a dense and continuous coverage in time. The selection of *N* and T_w-values does not affect the results in any way and they are changed in order to improve the quiescence signal. All details for these types of input parameters used in ZMAP program and some properties about the study areas are given in Table 2.

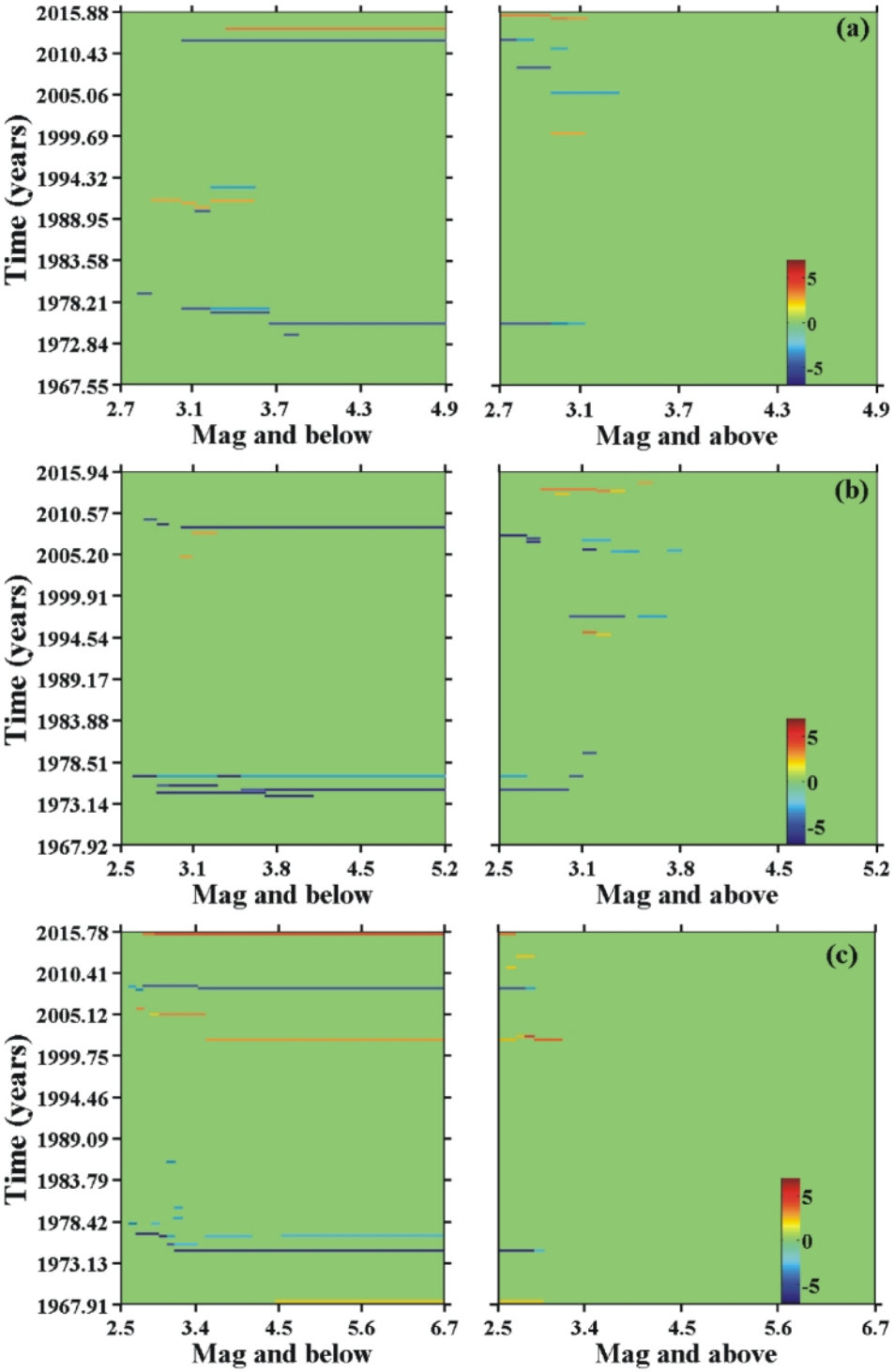

Figure 12: Results of *GENAS* estimates for declustered events for: the south western part (region 1), (b): the middle part (region 2), and (c): the north eastern part (region 3) of the VLED fault zone. Times of significant changes (at the 99% confidence level) are marked in blue for seismicity rate increases and in red for seismicity rate decreases as a function of different magnitude groups.

The regional distribution of the *Z*-value for the south western part (region 1) of the VLED fault zone is given in Figure 11a, indicating one seismic quiescence region (A). Two regions seismic quiescence (B and C) are observed in the middle part (region 2) of the VLED fault zone (Fig. 11b). In the north eastern part (region 3) three regions (D, E and F) show seismic quiescence anomalies (Fig. 11c).

For *Z*-value maps, the time window length for all regions is computed by adding T_w-value to the time chosen as the beginning of the time cut and so, Z-value changes for all regions are mapped for the same time, the beginning of 2016. In region 1, including the south western part of the VLED fault zone, the quiescence anomaly is centered at 40.81°N-19.86°E (region A, including Kuc-Bubullim, southeast of Lushnja town). In region 2, including the middle part of the VLED fault zone, the first anomaly region is centered at 41.00°N-20.01°E (region B, including Cerriku, south of Elbasani town) and the second one is centered at 41.31°N-20.13°E (regions C, including Bene-Qafe, northeast of Elbasani town). In region 3, including the north eastern part of the VLED fault zone, the first anomaly is centered at 41.43°N-20.21°E (region D, including Krasta-Batra, south of Bulqiza town), the second one is centered at 41.28°N-20.49°E (region E, including Carrishta-Stebleve, northeast of Librazhdi town), and the third one is centered at 41.51°N-20.51°E (region F, including Qerrenec-Gjorica, west of Dibra town).

In recent years, many authors such as Katsumata and Kasahara (1999), Chouliaras and Stavrakakis (2000), Polat et al., (2008), Öztürk, (2013; 2015), Öztürk and Bayrak (2012) achieved some quiescence analysis for different parts of the world and they detected significant seismic quiescence before the main shocks in their study regions. Thus, observed quiescence anomalous regions in different parts of the VLED fault zone may be significant and point out the next earthquake locations.

In addition to these statistical analysis, we used the *GENAS* technique (Habermann, 1983) in order to put forth all important rate changes of earthquake activity in different parts of the VLED fault zone. The *GENAS* algorithm estimates the cumulative numbers of different magnitude thresholds. In order to separate the magnitude groups where significant variations occur, the magnitude groups are separately evaluated. *GENAS* test is based on the iterative comparison of the earthquake activity rates at different magnitude thresholds (Zúñiga et al., 2000). The aim of the evaluating the numbers of magnitude groups separately is to see clearly the individual changes which occur in different magnitude groups. In short, the *GENAS* application describes the important variations in the number of earthquakes larger and smaller than a given magnitude versus time. *GENAS* algorithm defines the times which stand out as the start of periods were increases and/or decreases of earthquake activity can be identified as well as the magnitude range affected by these variations (Zúñiga et al., 2000; Chouliaras, 2009). Results of the *GENAS* model show the important breaks in slope which begin from the end of data for all magnitude groups. Here, "mag and below" states all earthquakes having a magnitude lower than M_D-value and, "*mag and above*" refers all event having a magnitude greater than M_D-value. The *GENAS* method hypothesized that only independent earthquakes can be compared in order to avoid false alarms from seismicity rate changes due to foreshock and aftershock sequences or clusters (Chouliaras, 2009). For this reason, we used the declustered earthquake catalogue for *GENAS* analysis.

The *GENAS* results (Fig. 12) indicate two significant increases in recorded small earthquakes and two clear decreases in recorded large events in 1975 and 2012 for the south western part (region 1, Fig. 12a) of the VLED fault zone. On the contrary, a massive decrease is reported for small earthquakes in 2014 and, some slight increases and decreases from 1990 to 1993. Also, there is a decreasing trend in large earthquakes in 2015. *GENAS* results for the middle part (region 2) of the VLED fault zone (Fig. 12b) indicate two strong increases in recorded small earthquakes between 1975 and 1977. A few weak variations of recorded large earthquakes are also observed for region 2 in 1975, 1997 and 2014, and also from 2004 to 2008. *GENAS* results for the north eastern part of the VLED fault zone (region 3) three strong increases in reported small earthquakes are pronounced in 1974, 1976 and 2008 (Fig. 12c). There are three strong decreases in reported small earthquakes and three small decreases in reported large events in 1968, 2001 and 2015. Two small increases in region 3 are also observed in recorded large earthquakes in 1974 and 2008. As an important result, we observed a remarkable compatibility between the results of seismic quiescence (Fig. 11) and the *GENAS* results (Fig. 12) at the beginning of 2016.

For a given region in different parts of the world, regional and spatial behaviors of earthquake activity have been evaluated in numerous studies and many different statistical methods have been used to make a detailed assessment of earthquake hazard. In recent years, many authors have used the combination of several statistical parameters such as Gutenberg-Richter *b*-value, correlation dimension *Dc*-value and precursory seismic quiescence *Z*-value in order to reveal the possible locations of future earthquakes in a given region (e.g., Wiemer and Wyss, 1994; Wyss and Martirosyan, 1998; Katsumata and Kasahara, 1999; Öncel and Wilson, 2002; Chouliaras and Stavrakakis, (2000); Huang et al., (2002); Wyss et al., 2004; Polat et al., 2008; Roy et al., 2011; Öztürk and Bayrak, 2012; Öztürk, 2011; 2013; 2015; Ali, 2016). The basic idea of these types of studies is that the regions with the lower *b*-value, the larger *Dc*-value and the higher *Z*-value are probable areas for next earthquake hazard. For example, an analysis on the evaluation of seismic hazard for the western part of Turkey is made by Polat et al. (2008) by using *b*-value and *Z*-value. They used the maximum likelihood approach to estimate the *b*-value and LTA (*t*) function to map the *Z*-value. They stated that the areas with the smaller *b*-value or larger *Z*-value can be interpreted as the most likely region for the next strong earthquake. Öztürk (2011) and Öztürk and Bayrak (2012) evaluated the seismic hazard potential of different parts of Turkey using such kind of parameters. Two large earthquakes

occurred in the eastern part of Turkey: March 8, 2010 Elazığ and October 23, 2011 Lake Van earthquakes. They observed some significant quiescence anomalies before the occurrence of these two earthquakes in 2010 and 2011 and, they observed their quiescence anomalies in and around the epicentral regions of these earthquakes. In short, these statistical parameters may be used in the forecasting of future earthquake locations. Because of the lower *b*-value, the larger *Dc*-value and the recent quiescence in several regions in and around the VLED fault zone at the beginning of 2016, these anomaly regions are important in the evaluation of seismic potential and hazard.

6. Conclusions

In the scope of this study, temporal and regional analyses of the recent earthquake activity in different parts of the Vlora-Lushnja-Elbasani-Dibra Transversal Fault Zone, Albania, are achieved. Several statistical parameters such as the Gutenberg-Richter *b*-value, the correlation dimension *Dc*-value and the precursory seismic quiescence *Z*-value as well as the regional, temporal and magnitude histograms of earthquake distributions were used in order to make a comprehensive evaluation for the earthquake hazard potential along the VLED fault zone. We used a homogeneous catalogue for duration magnitude, M_D and it includes 2814 earthquakes with $1.7 \leq M_D \leq 6.7$ for shallow earthquakes (<70 km) between July 20, 1967 and December 26, 2015. For the analysis of standard normal deviate *Z*-value, the earthquake catalogues for each region were declustered by using Reasenberg's algorithm.

The properties of earthquake distributions for different parts of the VLED fault zone are approximately the same and seismicity in all parts has an increasing trend gradually, especially after 1980. *Mc*-value estimations show a value of 2.7 for the south western part and 2.5 for the middle and north eastern part of the study region. Estimated *b*-values in all parts are around 1.0 and this is a characteristic value for earthquake catalogues. However, the north eastern part of the VLED zone has a *b*-value of 0.97 and this small value may be related to the increasing shear stress at the beginning of 2016. The *b*-value variations in time provide significant results and significant decreases are observed before the occurrences of strong earthquakes. A remarkable fact, this type of pioneering findings may be an evidence for the future strong main shocks. *Dc*-values for all parts are estimated as greater than 2.0, with 2.66 and 2.64 for the south western and middle parts, respectively. These large values mean that earthquake activity in these parts of the VLED fault zone are more clustered in smaller areas or larger scales.

Using the declustered earthquake catalogue, the regional distribution of *Z*-values is plotted in a grid space of 0.01° in latitude and longitude. We used a moving time window as T_w=5.5 years and observed several significant seismic quiescence regions at the beginning of 2016. In the south western part of the VLED fault zone, one quiescence anomaly is centered at 40.81°N-19.86°E. In the middle part of the VLED fault zone, the first anomaly is centered at 41.00°N-20.01°E and the second one is centered at 41.31°N-20.13°E. In the north eastern part of the VLED fault zone, one anomaly is centered at 41.43°N-20.21°E, the second one is centered at 41.28°N-20.49°E, and the third one is centered at 41.51°N-20.51°E.

There are many strong main shocks in the last 95 years in VLED fault zone, especially the recent 2009, 2014 and 2015 earthquakes. When considering the regions which have small *b*-value and large *Dc*-value with high Z-value, one can interpret that these anomaly regions may be interpreted as the possible locations of the next earthquakes. Hence, the combination of these types of seismotectonic variables and assessment of the regional and temporal behaviors together provides significant evidences in the identification of the seismic potential in and around the VLED fault zone. For this reason, further statistical analyses in this region will be useful, and the evaluations of *b*-value, *Dc*-value and *Z*-value with together may supply significant information for the forecasting of the next earthquake location and for the evaluation of seismic hazard in the VLED fault zone.

Acknowledgements

I would like to thank to Prof. Dr. Stefan Wiemer for providing ZMAP software. I also thank to the editor, reviewers Ewald Brückl and Sabine Hruby-Nichtenberger, for their useful and constructive comments, discussions and suggestions in improving this paper.

References

Aki, K., 1965. Maximum likelihood estimate of *b* in the formula log *N=a-bM* and its confidence limits. Bulletin of the Earthquake Research Institute, Tokyo University, 43, 237-239.

Ali, S.M., 2016. Statistical analysis of seismicity in Egypt and its surroundings. Arabian Journal of Geosciences, 9 (52), 2-16. http://dx.doi.org/10.1007/s12517-015-2079-x.

Aliaj, S.H., Sulstarova, E., Muço, B. and Kociu, S., 2001. Seismotectonic map of Albania, scale 1:500.000. Seismological Institute, Tirane.

Arabasz, W.J. and Hill, S.J., 1996. Applying Reasenberg's cluster analysis algorithm to regional earthquake catalogs outside California (abstract). Seismological Research Letters, 67(2), p. 30.

Awad, H., Mekkavi, M., Hassib, G. and Elbohoty, M., 2005. Temporal and three dimensional spatial analysis of seismicity in the Lake Aswan area, Egypt. Acta Geophysica Polonica 53 (2), 152-166.

Barton, D.J., Foulger, G.R., Henderson, J.R. and Julian, B.R., 1999. Frequency-magnitude statistics and spatial correlation dimensions of earthquakes at Long Valley Caldera, California. Geophysical Journal International, 138, 563–570. http://dx.doi.org/ 10.1046/j.1365-246X.1999.00898.x.

Chouliaras, G. and Stavrakakis, G.N., 2001. Current seismic quiescence in Greece: Implications for seismic hazard. Jour-

nal of Seismology, 5 (4), 595-608. http://dx.doi.org/10.1023/A:1012025024887.

Chouliaras, G., 2009. Investigating the earthquake catalog of the National Observatory of Athens, Natural Hazards Earth System Sciences, 9, 905-912. http://dx.doi.org/10.5194/nhess-9-905-2009.

Frohlich, C. and Davis, S., 1993. Teleseismic b-values: Or, much ado about 1.0. Journal of Geophysical Research, 98 (B1), 631-644. http://dx.doi.org/10.1029/92JB01891.

Goltz, C., 1998. Fractal and chaotic properties of earthquakes (Lecture Notes in Earth Sciences, 77), Springer-Verlag, 178 pp.

Grassberger, P. and Procaccia, I., 1983. Measuring the strangeness of strange attractors, Physica, 9(D), 189–208.

Gutenberg, R. and Richter, C.F., 1944. Frequency of earthquakes in California. Bulletin of the Seismological Society of America, 34, 185-188.

Habermann, R.E., 1983. Teleseismic detection in the Aleutian Island arc. Journal of Geophysical Research. 88 (B6), 5056-5064. http://dx.doi.org/10.1029/JB088iB06p05056.

Hirata, T., 1989. Correlation between the *b*-value and the fractal dimension of earthquakes. Journal of Geophysical Research. 94, 7507-7514. http://dx.doi.org/10.1029/JB094iB06p07507.

Huang, Q., Öncel, A.O. and Sobolev, G.A., 2002. Precursory seismicity changes associated with the MW=7.4 1999 August 17 Izmit (Turkey) earthquake. Geophysical Journal International, 151, 235-242.

Kagan, Y.Y., 2007. Earthquake spatial distribution: the correlation dimension. Geophysical Journal International, 168, 1175-1194. http://dx.doi.org/10.1111/j.1365-246X.2006.03251.x.

Katsumata, K. and Kasahara, M., 1999. Precursory seismic quiescence before the 1994 Kurile earthquake (M_w = 8.3) revealed by three independent seismic catalogs. Pure and Applied Geophysics. 155, 2-4, 443-470. http://dx.doi.org/10.1007/s000240050274.

Kociaj, S., 1986. The risk of the Albanian's earth crust and its specification for the ground construtsion. PhD thesis, Tirana.

Mandelbrot, B.B., 1982. The fractal geometry of nature. Freeman Press, San Francisco.

Mazzoli, S. and Helman, M., 1994. Neogene patterns of relative plate motion for Africa-Europe: some implications for recent central Mediterranean tectonics. Geologische Rundschau, 83, 464-468.

Melo, V., 1986. The structural geology and geotectonic (The geology of the Albanides) (In Albanian). The Publishing House of University of Tirana.

Mogi, K., 1962. Magnitude-frequency relation for elastic shocks accompanying fractures of various materials and some related problems in earthquakes. Bulletin of the Earthquake Research Institute, Tokyo University, 40, 831-853.

Olsson, R., 1999. An estimation of the maximum b-value in the Gutenberg-Richter relation. Geodynamics, 27, 547–552.

Ormeni, Rr., 2007. The general model of construction of the Albanian earth crust and its seismoactive feature according to the seismological data. PhD thesis, Tirana, Albania.

Ormeni, Rr., 2010. Structure of P, S seismic wave velocities of the Albanian earth lithospheres and its seismoactive features. Kumi publications, Tirana.

Ormeni, Rr. Kociaj, S., Fundo, A., Daja, S.H. and Doda, V., 2013. Moderate earthquakes in Albania during 2009 and their associated seismogenic zones. Italian Journal of Geosciences, 132 (2), 203-212. http://dx.doi.org/10.3301/IJG.2012.45.

Ormeni, Rr., 2015. Mapping *b*-value in the seismogenic zones of Albania region. Proceeding of the 8th Congress of the Balkan Geophysical Society, 4-8 October 2015, Crete, Greece.

Öncel, A.O. and Wilson, T.H., 2002. Space-time correlations of seismotectonic parameters and examples from Japan and Turkey preceding the İzmit earthquake. Bulletin of the Seismological Society of America, 92, 339-350. http://dx.doi.org/10.1785/0120000844.

Öncel, A.O. and Wilson, T.H., 2007. Anomalous seismicity preceding the 1999 Izmit event, NW Turkey. Geophysical Journal International, 169, 259-270. http://dx.doi.org/10.1111/j.1365-246X.2006.03298.x.

Öztürk, S., Bayrak, Y., Çinar, H., Koravos, G.Ch. and Tsapanos, T.M. 2008. A quantitative appraisal of earthquake hazard parameters computed from Gumbel I method for different regions in and around Turkey. Natural Hazards 47, 471-495. http://dx.doi.org/10.1007/s11069-008-9234-6.

Öztürk, S., 2011. Characteristics of Seismic Activity in the Western, Central and Eastern Parts of the North Anatolian Fault Zone, Turkey: Temporal and Spatial Analysis. Acta Geophysica, 59 (2), 209-238. http://dx.doi.org/10.2478/s11600-010-0050-5.

Öztürk, S. and Bayrak, Y., 2012. Spatial variations of precursory seismic quiescence observed in recent years in the eastern part of Turkey. Acta Geophysica, 60 (1), 92-118. http://dx.doi.org/10.2478/s11600-011-0035-z.

Öztürk, S., 2013. A statistical assessment of current seismic quiescence along the North Anatolian Fault Zone: Earthquake precursors. Austrian Journal of Earth Sciences, 106 (2), 4-17.

Öztürk, S., 2015. A study on the correlations between seismotectonic *b*-value and *Dc*-value, and seismic quiescence *Z*-value in the Western Anatolian region of Turkey. Austrian Journal of Earth Sciences, 108 (2), 172-184. http://dx.doi.org/10.17738/ajes.2015.0019.

Prasad, S. and Singh, C., 2015. Evolution of b-values before large earthquakes of m_b>6.0 in the Andaman region. Geologica Acta, 13(3), 205-210. http://dx.doi.org/10.1344/ GeologicaActa2015.13.3.3.

Polat, O., Gok, E. and Yılmaz, D., 2008. Earthquake hazard of the Aegean Extension region (West Turkey), Turkish Journal of Earth Sciences, 17, 593-614.

Reasenberg, P.A., 1985. Second-order moment of Central California seismicity, 1969-1982. Journal of Geophysical Research, 90 (B7), 5479-5495. http://dx.doi.org/10.1029/JB090iB07p05479.

Roy, S., Ghosh, U., Hazra, S. and Kayal, J.R., 2011. Fractal dimension and b-value mapping in the Andaman-Sumatra subduc-

tion zone. Natural Hazards, 57, 27–37. http://dx.doi.org/10.1007/s11069-010-9667-6.

Scholz, C.H., 1968. The frequency-magnitude relation of microfracturing in rock and its relation to earthquakes. Bulletin of the Seismological Society of America, 58, 399-415.

Sulstarova, E., and Kociaj, S., 1975. Catalog of earthquakes of Albania. Published, Science Academy of Albania, Tirane.

Sulstarova, E., Kociaj, S., and Aliaj, S.H., 1980. Seismic Regionalizition of Albania. Published, Science Academy of Albania, Tirane.

Sulstarova, E., Peçi, V. and Shuteriqi, P., 2000. Vlora-Elbasani-Dibra (Albania) transversal fault zone and its seismic activity. Journal of Seismology, 4, 117-131.

Toksöz, M.N., Shakal, A.F. and Michael, A.J., 1979. Space-time migration of earthquakes along the North Anatolian Fault Zone and seismic gaps. Pure and Applied Geophysics, 117, 1258–1270.

Utsu, T., 1971. Aftershock and earthquake statistic (III): Analyses of the distribution of earthquakes in magnitude, time and space with special consideration to clustering characteristics of earthquake occurrence (1). Journal of Faculty of Science, Hokkaido University, Series VII (Geophysics), 3, 379-441.

Wang, J.H., Chen, K.C., Leu, P.L. and Chang, C.H., 2016. Precursor times of abnormal b-values prior to mainshocks. Journal of Seismology, 20, 905-919. http://dx.doi.org/10.1007/s10950-016-9567-7.

Wiemer, S. and Wyss, M., 1994. Seismic quiescence before the Landers (M=7.5) and Big Bear (6.5) 1992 earthquakes. Bulletin of the Seismological Society of America, 84 (3), 900-916.

Wiemer, S. and Wyss, M., 2000. Minimum magnitude of completeness in earthquake catalogs: Examples from Alaska, the Western United States, and Japan. Bulletin of the Seismological Society of America, 90 (3), 859-869. http://dx.doi.org/10.1785/0119990114.

Wiemer, S., 2001. A software package to analyze seismicity: ZMAP. Seismological Research Letters, 72(2), 373-382. http://dx.doi.org/10.1785/gssrl.72.3.373.

Woessner, J. and Wiemer, S., 2005. Assessing the quality of earthquake catalogues: Estimating the magnitude of completeness and its uncertainty. Bulletin of the Seismological Society of America, 95 (2), 684-698. http://dx.doi.org/10.1785/0120040007.

Wyss, M. and Martirosyan, A.H., 1998. Seismic quiescence before the M7, 1988, Spitak earthquake, Armenia, Geophysical Journal International, 134, 2, 329-340. http://dx.doi.org/10.1046/j.1365-246x.1998.00543.x.

Wyss, M., Sobolev, G.A. and Clippard, J.D., 2004. Seismic quiescence precursors to two M7 earthquakes on Sakhalin Island, measured by two methods, Earth Planets Space, 56, 725-740.

Zúñiga, R.F., Reyes, M.A. and Valdés, C., 2000. A general overview of the catalog of recent seismicity compiled by the Mexican Seismological Survey, Geofísica Internacional, 39 (2), 161-170.

Received: 22 July 2017
Accepted: 13 November 2017

Rrapo ORMENI[1)], Serkan ÖZTÜRK[2)*)], Akli FUNDO[3)] & Kemal ÇELIK[4)]

[1)] Institute of Geosciences, Energy, Water and Enivornment Polytechnic University, Tirana, Albania;

[2)] Gümüşhane University, Department of Geophysics, TR-29100, Gümüşhane, Turkey;

[3)] Polytechnic University, Tirana, "Nene Tereza" square, Albania;

[4)] Gümüşhane University, Department of Geomatics Engineering, TR-29100, Gümüşhane, Turkey;

[*)] Corresponding author, serkanozturk@gumushane.edu.tr